Occupancy Estimation Using Only WiFi Power Measurements

Saandeep Depatla, Arjun Muralidharan and Yasamin Mostofi

***Abstract*—In this paper, we are interested in counting the total number of people walking in an area based on only WiFi received signal strength indicator (RSSI) measurements between a pair of stationary transmitter/receiver antennas. We propose a framework based on understanding two important ways that people leave their signature on the transmitted signal: blocking the Line of Sight (LOS) and scattering effects. By developing a simple motion model, we first mathematically characterize the impact of the crowd on blocking the LOS. We next probabilistically characterize the impact of the total number of people on the scattering effects and the resulting multipath fading component. By putting the two components together, we then develop a mathematical expression for the probability distribution of the received signal amplitude as a function of the total number of occupants, which will be the base for our estimation using Kullback-Leibler divergence. In order to confirm our framework, we run extensive indoor and outdoor experiments with up to and including 9 people and show that the proposed framework can estimate the total number of people with a good accuracy with only a pair of WiFi cards and the corresponding RSSI measurements.**

***Index Terms*—Occupancy counting, WiFi measurements, Crowd counting, Probabilistic Analysis**

I. Introduction

In recent years, there has been considerable interest in understanding what WiFi signals can tell us about our environment. There are several potential applications that can benefit from such a sensing that relies only on the available WiFi signals. Search and rescue [1], robotic exploration, location-aware services, and smart health systems such as elderly monitoring, are just a few examples.

Work on WiFi-based localization can be broadly categorized into two groups: device-based active and device-free passive localization. A survey of the literature shows several work in the area of device-based sensing and localization, where a user's WiFi-enabled gadget, for instance, actively tries to position itself [2], [3]. In passive device-free sensing, on the other hand, WiFi-enabled nodes/network sense and map their environment, for instance objects and humans, without any communication from those objects. Along this line, there has been work on seeing through walls with only WiFi (our past work) [1], [4], motion tracking [5], [6], and gesture recognition [7].

In this paper, we are interested in occupancy estimation, i.e. estimating the total number of people walking in a given space, based on only WiFi power measurements between a transmitter and a receiver. Fig. 1 shows an example of our considered scenario, where a fixed TX/RX pair are tasked with estimating the total number of people that are casually walking in an area.

There are several potential applications that can benefit from occupancy estimation. Smart building management, where heating and cooling can be automatically optimized based on detecting the level of occupancy is one example, which can result in a considerable energy saving [8], [9]. There are other similar location-aware services that a business can also optimize based on detecting the level of occupancy. Proper occupancy detection can also play a key role in an emergency response operation where a crowd needs to be guided to evacuate an area.

Current literature on occupancy level detection either uses cameras [10]–[12] or RF signals. The use of direct vision-based techniques (cameras) is typically limited by high deployment and computational costs. Occupancy detection, based on RF signals, on the other hand, has recently attracted considerable attention. Several methods in this category, however, are active and rely on RF devices carried by users, which may not be feasible [13]–[15]. Along the line of device-free RF-based occupancy estimation, another line of work has relied on the use of a network of RF nodes (e.g. 10-20 nodes) and fingerprinting/prior site surveys for classification based on received signal strength (RSS) measurements [16]. In [17], multiple RF nodes are used to estimate the location and total number of up to four people based on RSS measurements. They report accuracy within an estimation error of 1 person, approximately 84% of the time. [18] uses a similar approach with fewer nodes and counts up to three people. In [19], a TX/RX pair is used to detect the number of people based on RSS measurements. Extensive training data is used (at the level of running the real experiment) to develop the underlying model and errors up to six people are reported in a study limited to 9 people. In [20], the authors measure the channel state information across several sub-carriers (e.g. 30), develop a model to relate this to the total number of people through a training phase, and test their approach with one transmitter and three receivers, for counting up to and including 9 people. However, measuring channel state across several frequency sub-bands is not possible with most current WiFi cards. In [21], authors use ultrawideband radar to count up to three stationary people behind walls, based on vital signal detection. In [22], the authors use a pulsed radar for occupancy estimation by applying learning algorithms.

In this paper, we are interested in estimating the total number of people walking in an area based on only WiFi power measurements (no channel state measurements at several sub-carriers required) between only one fixed TX/RX pair, as shown in Fig. 1. As we shall see, through a proper

This work is supported in part by NSF CAREER award # 0846483.

The authors are with the Department of Electrical and Computer Engineering, University of California Santa Barbara, Santa Barbara, CA 93106, USA email: {saandeep, arjunm, ymostofi}@ece.ucsb.edu.

mathematical characterization of the blocking and multipath fading effects, we can count up to and including 9 people in both indoor and outdoor environments with a good accuracy. To the best of our knowledge, a similar performance has not been reported before with only RSSI measurements. For instance, [20] uses channel state measurements across 30 sub-channels and three receivers to achieve a similar performance. This holds promises for further extension of the state of the art on occupancy detection. For instance, if one can also measure the channel state at several sub-carriers, this additional information and our probabilistic approach can potentially be combined to achieve a good quality occupancy detection in more complex areas with a higher number of people.

Next, we summarize our key contributions. We separate the impact of a walking person on the transmitted WiFi signal into two key components: 1) blocking of the LOS and 2) multipath effect. This separation is important as each component carries information on the total number of people in a different way. By developing a simple motion model, we then mathematically characterize the first component probabilistically. Our results indicate that this component carries vital information on the total number of people. For instance, if directional antennas are used, this component could even suffice for high-accuracy occupancy estimation (at least for up to and including 9 people), as our experimental results confirm. We further characterize the scattering impact of people through probabilistically analyzing the resulting multipath fading as a function of the number of occupants. By putting the two components together, we finally develop a mathematical expression for the probability distribution of the received signal amplitude as a function of the total number of occupants. This derived PDF is then compared to the experimental one via using Kullback-Leibler divergence as a metric, and the argument that minimizes it is taken as the estimate of the number of occupants. We then run extensive indoor and outdoor experiments with up to and including 9 people and both omni and directional antennas. Our results confirm that the proposed framework can estimate the total number of walking people with a good accuracy. For instance, an error of 2 or less is achieved 96% and 63% of the time for the outdoor and indoor cases respectively, when using the typical omnidirectional antennas that come as part of the standard WiFi cards. When using directional antennas, we further observe an error of 2 or less 100% of the time for both the outdoor and indoor cases.

The rest of the paper is organized as follows. In Section II, we explain our problem formulation and develop our motion model. In Section III-A, we characterize the probability of crossing the LOS. Multipath effects are then modeled in Section III-B, where a final expression is developed by putting both blocking and multipath effects together. In Section IV, we present several indoor and outdoor experimental results confirming that our approach can estimate the total number of people with a good accuracy. We conclude and discuss further extensions in Section V.

Fig. 1: A stationary WiFi transmitter and receiver are tasked with determining the number of people in the area based on the received power measurements over a short period of time. Note that the robots are merely carrying the WiFi cards and TX/RX are not moving in this paper.

II. Problem Formulation

Consider a scenario where N people are walking casually in an area as shown in Fig. 1. A WiFi transmitter (TX) and receiver (RX) are positioned (both stationary) at the border of this area to collect measurements, as marked in the figure. The goal of this paper is to estimate the total number of people based on only the received signal strength measurements over a small period of time. In this section, we present the mathematical formulation of our motion model. It should be noted that in our experiments, we have no control over how people walk and they are simply asked to walk casually. Thus, the purpose of this section is to derive a simple mathematical model for a casual walk.

A. Workspace Model

Consider a rectangular region of dimension $L \times B$, as shown in Fig. 2a. We discretize it to form a 2-D discrete workspace $\mathcal{W}$ consisting of cells, wherein the position of each cell is specified by the coordinates of its center. The origin is taken to be at the lower left corner. Moreover, the length and breadth are partitioned into $N_{\text{div},x}$ and $N_{\text{div},y}$ segments respectively. The dimension of a cell is thus $\Delta x \times \Delta y$, with $\Delta x = L/N_{\text{div},x}$ and $\Delta y = B/N_{\text{div},y}$. The workspace can then be summarized by $\mathcal{W} = \{(x,y)|x \in \mathcal{X}, y \in \mathcal{Y}\}$ where $\mathcal{X} = \{\frac{1}{2}\Delta x, \frac{3}{2}\Delta x, \cdots \frac{2N_{\text{div},x}-1}{2}\Delta x\}$ and $\mathcal{Y} = \{\frac{1}{2}\Delta y, \frac{3}{2}\Delta y, \cdots \frac{2N_{\text{div},y}-1}{2}\Delta y\}$.

A transmitter and receiver are located at the coordinates $(L/2, 0)$ and $(L/2, B)$ respectively. N people are moving in this workspace. In our mathematical modeling of this section, we discretize the position of each person to the center of a cell. This is solely for modeling purposes and people are not walking in a discretized manner in our experimental setup.

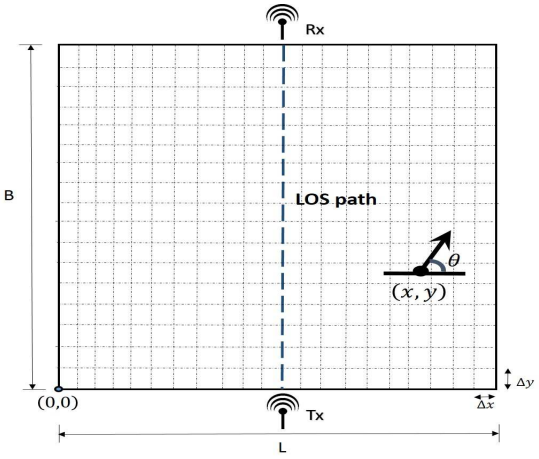

(a)

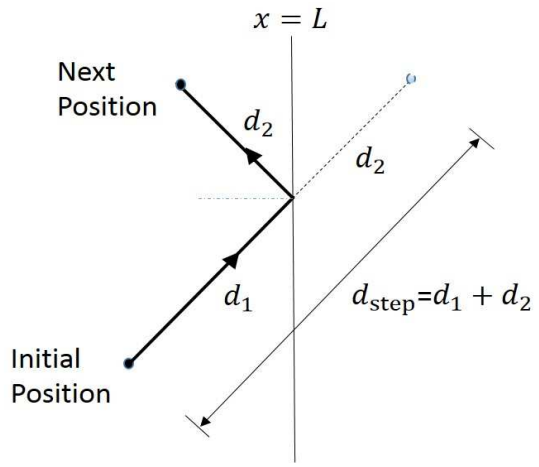

(b)

Fig. 2: (a) An illustration of the workspace, (b) An illustration of the modeled boundary behaviour.

B. Motion Model

In general, mathematical modeling of the motion of people is a challenging problem and not the focus of this paper. Instead, we are interested in a simple probabilistic motion model in order to characterize the stationary distribution of the position/heading of the people in the next section.

In our experiments, people were asked to walk casually. We observed that people had a tendency to maintain their direction for a while before changing it. In this section we come up with a simple mathematical model to characterize the movement of the people. For the sake of mathematical characterization, we assume that each person moves around the workspace independent of the others and at a speed of d_{step} per iteration.[1] At each iteration, we assume that a person chooses a direction θ (w.r.t the x axis as shown in Fig. 2a) and moves a distance of d_{step} in that direction. If a step results in a person crossing the boundary, we assume that the person reflects off the boundary and lands back inside the workspace, as shown in Fig. 2b. Note that the total distance traveled is still d_{step}, as shown in Fig. 2b. At every iteration, the position of a person would be quantized to the center of the cell in which she currently resides.

We discretize the angle space $[0, 2\pi)$ into $\vartheta = \{0, \Delta\theta, \cdots, (N_{\text{div},\theta} - 1)\Delta\theta\}$ with $\Delta\theta = \frac{2\pi}{N_{\text{div},\theta}}$. At each iteration, we assume that each person maintains the same heading of the previous iteration, i.e. chooses the same θ, with the probability $p_\theta < 1$, and selects an angle uniformly from ϑ with the probability $1 - p_\theta$. The motion of person i can then be characterized by the following,

$$\theta_i(t+1) = \begin{cases} \theta_i(t) & \text{w.p. } p_\theta \\ \text{uniformly from } \vartheta & \text{w.p. } 1 - p_\theta \end{cases}, \tag{1}$$

$$x_i(t+1) = \begin{cases} -x_i(t) - \text{round}_x(d_{\text{step}} \cos\theta_i(t)) \\ \quad \text{if } x_i(t) + \text{round}_x(d_{\text{step}} \cos\theta_i(t)) < 0 \\ 2L - x_i(t) - \text{round}_x(d_{\text{step}} \cos\theta_i(t)) \\ \quad \text{if } x_i(t) + \text{round}_x(d_{\text{step}} \cos\theta_i(t)) > L \\ x_i(t) + \text{round}_x(d_{\text{step}} \cos\theta_i(t)) \\ \quad \text{otherwise} \end{cases}, \tag{2}$$

$$y_i(t+1) = \begin{cases} -y_i(t) - \text{round}_y(d_{\text{step}} \sin\theta_i(t)) \\ \quad \text{if } y_i(t) + \text{round}_y(d_{\text{step}} \sin\theta_i(t)) < 0 \\ 2B - y_i(t) - \text{round}_y(d_{\text{step}} \sin\theta_i(t)) \\ \quad \text{if } y_i(t) + \text{round}_y(d_{\text{step}} \sin\theta_i(t)) > B \\ y_i(t) + \text{round}_y(d_{\text{step}} \sin\theta_i(t)) \\ \quad \text{otherwise} \end{cases}, \tag{3}$$

where $\text{round}_x(d) = (\arg\min_{k\in\mathbb{Z}} |d - k\Delta x|)\Delta x$ and $\text{round}_y(d) = (\arg\min_{k\in\mathbb{Z}} |d - k\Delta y|)\Delta y$ are functions that round the input to the closest multiple of Δx and Δy respectively. Furthermore $x_i(t)$ and $y_i(t)$ denote the position of the i^{th} person at time t along the x and y axis respectively, and $\theta_i(t)$ represents the angle of person i at time t. Note that we excluded the case of $p_\theta = 1$ as it implies a purely deterministic motion model, which is not a good representation of a casual walk.

III. Estimation of the Total Number of People Based on WiFi Power Measurements

In this section, we discuss our proposed approach for estimating the total number of people based on only WiFi power measurements. A person will leave her signature on the received signal in two ways. First, when she crosses the LOS path between the TX and RX, she blocks the transmitted signal, resulting in a drop in the received signal power. Second, she acts as a scatterer of the signal, contributing to multipath fading (MP). As a result, we have two underlying effects: possible blockage of the LOS and multipath fading, both of which carry implicit information of N. Fig. 3 shows an example of a received signal power measurement (N=5 in this case). Sample arrows on the figure mark the impact of LOS blockage as well as MP. For a lower level of occupancy, the blocking effect typically results in more pronounced drops as compared to MP. However, as the number of people increases, MP can result in similar levels of drop. As such, it is important to consider both effects.

[1] An iteration refers to a time instant under the discretization of time.

Our proposed approach is thus based on the understanding and characterization of the impact of N on these two phenomena.[2] We start by modeling the probability of blocking the LOS path in Section III-A. This characterization is then utilized in Section III-B, to mathematically model both effects and find an expression for the overall probability density function (PDF) of the received signal amplitude as a function of N.

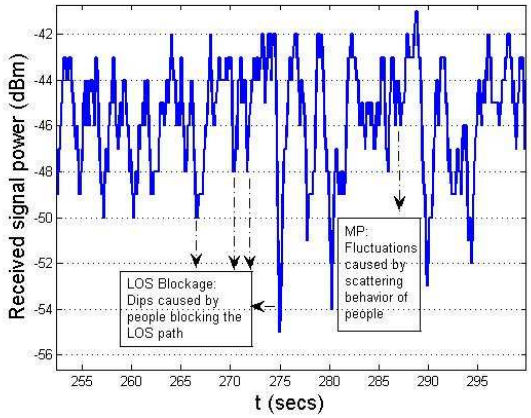

Fig. 3: Sample received signal power for N=5, where a few examples of LOS blocking and MP effects are marked.

A. Characterization of the Probability of Blocking the LOS

In this section we characterize the probability that k number of people cross the LOS in an iteration. We begin by finding the stationary probability distribution of the position and heading of a person. The main reason to characterize a stationary distribution is to make our framework as independent of the details of the motion as possible. We discuss this further in Remark 1. This, however, does not imply that we need to collect measurements for a very long period of time in practice. For instance, as we shall see in Section IV, we collect measurements for only 300 seconds, and the modeling of our paper provides a good approximation.

1) Asymptotic Distribution of the Position and Heading: In this part, we prove that the position and heading of a person takes a uniform distribution asymptotically.

Let $\Theta(t) \in \vartheta$ be a random variable denoting the heading of a person at time t. Equation (1) induces a Markov chain as follows:

$$\mu^{\Theta}(t+1) = P^{\Theta}\mu^{\Theta}(t), \tag{4}$$

where $\mu^{\Theta}(t)$ is a column vector with the i^{th} entry as $[\mu^{\Theta}(t)]_i = \Pr(\Theta(t) = (i-1)\Delta\theta)$ for $i \in \{1, 2, \cdots, N_{\text{div},\theta}\}$ and P^{Θ} is a matrix with the $(i,j)^{\text{th}}$ entry as $[P^{\Theta}]_{ij} = \Pr\Big(\Theta(t+1) = (i-1)\Delta\theta | \Theta(t) = (j-1)\Delta\theta\Big)$ for $i, j \in \{1, 2, \cdots, N_{\text{div},\theta}\}$.

Lemma 1: Consider the heading dynamics of (1). Then the stationary distribution of $\Theta(t)$ is uniform.

[2]We note that there are several propagation phenomena when a transmission occurs. Our goal is not to model all these effects but rather have a simple yet comprehensive enough modeling for the purpose of estimating N.

Proof: From the heading dynamics, we have the probability transition matrix as

$$P^{\Theta} = \begin{pmatrix} p_\theta + \frac{1-p_\theta}{N_{\text{div},\theta}} & \frac{1-p_\theta}{N_{\text{div},\theta}} & \cdots & \frac{1-p_\theta}{N_{\text{div},\theta}} \\ \frac{1-p_\theta}{N_{\text{div},\theta}} & p_\theta + \frac{1-p_\theta}{N_{\text{div},\theta}} & \cdots & \frac{1-p_\theta}{N_{\text{div},\theta}} \\ \vdots & \vdots & \ddots & \vdots \\ \frac{1-p_\theta}{N_{\text{div},\theta}} & \frac{1-p_\theta}{N_{\text{div},\theta}} & \cdots & p_\theta + \frac{1-p_\theta}{N_{\text{div},\theta}} \end{pmatrix}.^{3} \tag{5}$$

It can be seen that P^{Θ} is doubly stochastic. By applying the Geršgorin disk theorem [23], it can be easily seen that the spectral radius of P^{Θ} is 1. Since $p_\theta < 1$, we have $P^{\Theta} \succ 0$, i.e. P^{Θ} is positive. Then, by applying the Perron-Frobenius theorem [24], we have $\lim_{t\to\infty}(P^{\Theta})^t = \mathbf{1}_{N_{\text{div},\theta}}\omega^T$, where ω is the left eigenvector of P^{Θ}, $\mathbf{1}^T_{N_{\text{div},\theta}}\omega = 1$ and $\mathbf{1}_r$ denotes a column vector of ones of size r. It can be easily confirmed that $\omega = \frac{1}{N_{\text{div},\theta}}\mathbf{1}_{N_{\text{div},\theta}}$, since P^{Θ} is doubly stochastic, resulting in $\lim_{t\to\infty}(P^{\Theta})^t = \frac{1}{N_{\text{div},\theta}}\mathbf{1}_{N_{\text{div},\theta}}\mathbf{1}^T_{N_{\text{div},\theta}}$ and

$$\mu^{\Theta} = \lim_{t\to\infty}\mu^{\Theta}(t) = \frac{1}{N_{\text{div},\theta}}\mathbf{1}_{N_{\text{div},\theta}}. \tag{6}$$

This means that the heading takes a uniform distribution asymptotically. ■

We next characterize the asymptotic distribution of the position. Let $X(t) \in \mathcal{X}$ be a random variable denoting the x axis coordinate of a person at time t. Equation (2) then induces the following Markov chain,

$$\mu^X(t+1) = P^X\mu^X(t), \tag{7}$$

where $\mu^X(t)$ is a column vector with the i^{th} entry $[\mu^X(t)]_i = \Pr(X(t) = \frac{2i-1}{2}\Delta x)$, for $i \in \{1, \cdots, N_{\text{div},x}\}$, and P^X is a matrix with the $(i,j)^{\text{th}}$ entry as $[P^X]_{ij} = \Pr\Big(X(t+1) = \frac{2i-1}{2}\Delta x | X(t) = \frac{2j-1}{2}\Delta x\Big)$ for $i, j \in \{1, \cdots, N_{\text{div},x}\}$.

Lemma 2: Consider the motion dynamics of (1)-(3). Then, the stationary distribution of $X(t)$ is uniform.

Proof: Let $\Theta = \lim_{t\to\infty}\Theta(t)$. Let $D_x = \text{round}_x(d_{\text{step}}\cos\Theta)$ be a random variable denoting the distance traveled by a person (rounded to a multiple of Δx) along the x axis when the probability distribution of $\Theta(t)$ has converged to its stationary distribution. The probability mass function (PMF) of D_x, p_{D_x}, is given as

$$\begin{aligned} p_{D_x}(k\Delta x) &= \sum_{i\in\{1,\cdots,N_{\text{div},\theta}\}: d_{\text{step}}\cos(\frac{i-1}{N_{\text{div},\theta}}2\pi)\in[k\Delta x-\frac{\Delta x}{2}, k\Delta x+\frac{\Delta x}{2})} (\mu^{\Theta})_i \\ &= \sum_{i\in\{1,\cdots,N_{\text{div},\theta}\}: d_{\text{step}}\cos(\frac{i-1}{N_{\text{div},\theta}}2\pi)\in[k\Delta x-\frac{\Delta x}{2}, k\Delta x+\frac{\Delta x}{2})} \frac{\Delta\theta}{2\pi} \\ &\approx 2\int_{\theta\in[0,\pi): d_{\text{step}}\cos\theta\in[k\Delta x-\frac{\Delta x}{2}, k\Delta x+\frac{\Delta x}{2})} \frac{1}{2\pi}d\theta \\ &= \int_{k\Delta x-\frac{\Delta x}{2}}^{k\Delta x+\frac{\Delta x}{2}} \frac{1}{\pi\sqrt{d^2_{\text{step}} - r^2}}dr \\ &\approx \begin{cases} \frac{\Delta x}{\pi\sqrt{d^2_{\text{step}} - (k\Delta x)^2}}, & \text{if } k \in \mathbb{Z} \text{ and } |k\Delta x| < d_{\text{step}} \\ 0 & \text{else} \end{cases}, \end{aligned} \tag{8}$$

[3]An additional $\frac{1-p_\theta}{N_{\text{div},\theta}}$ term is present along the diagonal since a person may still select its previous angle when she selects uniformly from ϑ.

where the second equality follows since $[\mu^{\Theta}]_i = \frac{1}{N_{\text{div},\theta}} = \frac{\Delta\theta}{2\pi}$ for $i \in \{1, \cdots, N_{\text{div},\theta}\}$. Moreover, the fourth equality follows from the change of variable $r = d_{\text{step}} \cos\theta$.

The $(j,i)^{\text{th}}$ element of P^X can then be expressed as

$$\begin{aligned}
[P^X]_{ji} &= \Pr\left(X(t+1) = \frac{2j-1}{2}\Delta x | X(t) = \frac{2i-1}{2}\Delta x\right) \\
&= \begin{cases} p_{D_x}((j-i)\Delta x) + p_{D_x}((-j-i+1)\Delta x) \\ \qquad \text{if } j \in \{1, \cdots, \lfloor \frac{d_{\text{step}}}{\Delta x} \rfloor\} \\ p_{D_x}((j-i)\Delta x) + \\ \qquad p_{D_x}((2N_{\text{div},x}+1-j-i)\Delta x) \\ \qquad \text{if } j \in \{N_{\text{div},x} - \lfloor \frac{d_{\text{step}}}{\Delta x} \rfloor, \cdots, N_{\text{div},x}\} \\ p_{D_x}((j-i)\Delta x) \\ \qquad \text{else} \end{cases} \\
&= [P^X]_{ij},
\end{aligned} \tag{9}$$

where the second terms in the first and second cases denote the probability of a transition from the i^{th} to the j^{th} cell via reflections off of the boundaries, and the last line follows since $p_{D_x}(i\Delta x) = p_{D_x}(-i\Delta x)$. It can be seen that P^X is thus doubly stochastic. Moreover, the graph induced by P^X is strongly connected and aperiodic. This implies that P^X is primitive [25]. Thus, similar to (6), we can apply the Perron-Frobenius theorem to deduce that

$$\mu^X = \lim_{t\to\infty} \mu^X(t) = \frac{1}{N_{\text{div},x}} \mathbf{1}_{N_{\text{div},x}}. \tag{10}$$

■

A similar analysis can be carried out for the probability of the position along the y-axis. Lemma 1 and 2 show that the position and heading of a person takes a uniform distribution asymptotically.

Remark 1: While we derived the uniform asymptotic distribution for the angle model of (1), constant speed, and boundary behavior of Fig. 2b, we expect that an asymptotic stationary distribution will be achieved whenever there is a small amount of randomness in the motion model. A more rigorous characterization of this, however, is a subject of further studies.

2) Characterization of the Probability of Blocking: In this part, we derive a mathematical expression for the probability of blocking the LOS.

Definition 1: We say a blocking (crossing)[4] has occurred at time $t+1$ if either $x_i(t) \le L/2$ and $x_i(t+1) \ge L/2$ or $x_i(t) \ge L/2$ and $x_i(t+1) \le L/2$.

Based on the definition above, a cross has also occurred if a person lands exactly on the LOS path or moves along it. Thus, this probability of crossing considers slightly more cases than the case of only cutting the LOS, which is of interest to us. However, as we shall see, since we take $\Delta x \to 0$, the probability of these special cases tends to zero, resulting in the desired probability of crossing.

Theorem 1: The asymptotic probability of a cross of a single person in an iteration can be characterized as

$$p_{\text{cross}} = \frac{2d_{\text{step}}}{\pi L}. \tag{11}$$

[4]We use the terms crossing and blocking interchangeably since a non-zero speed is assumed.

Proof: A crossing occurs if a person who is sufficiently close to the LOS takes a large enough step to go over the LOS line. Based on Lemma 2, we can write the following expression for the probability of a cross of one person (in one time step):

$$\begin{aligned}
p_{\text{cross}} &= 2 \sum_{i=\lfloor \frac{L}{2\Delta x}+\frac{1}{2} \rfloor - \lfloor \frac{d_{\text{step}}}{\Delta x} \rfloor}^{\lfloor \frac{L}{2\Delta x}+\frac{1}{2} \rfloor} [\mu^X]_i \sum_{k=\lceil \frac{L}{2\Delta x}+\frac{1}{2} \rceil - i}^{\lfloor \frac{d_{\text{step}}}{\Delta x} \rfloor} p_{D_X}(k\Delta x) \\
&= 2 \sum_{i=\lfloor \frac{L}{2\Delta x}+\frac{1}{2} \rfloor - \lfloor \frac{d_{\text{step}}}{\Delta x} \rfloor}^{\lfloor \frac{L}{2\Delta x}+\frac{1}{2} \rfloor} \frac{\Delta x}{L} \\
&\qquad \sum_{k=\lceil \frac{L}{2\Delta x}+\frac{1}{2} \rceil - i}^{\lfloor \frac{d_{\text{step}}}{\Delta x} \rfloor} \frac{\Delta x}{\pi\sqrt{d_{\text{step}}^2 - (k\Delta x)^2}} \\
&\approx 2 \int_{L/2-d_{\text{step}}}^{L/2} \int_{L/2-x}^{d_{\text{step}}} \frac{1}{L} \frac{1}{\pi\sqrt{d_{\text{step}}^2 - (r)^2}} dx dr \\
&= 2 \int_0^{d_{\text{step}}} \frac{1}{L} \int_{x/d_{\text{step}}}^{1} \frac{1}{\pi\sqrt{1-r^2}} dx dr \\
&= \frac{2d_{\text{step}}}{\pi L},
\end{aligned} \tag{12}$$

where the second equality follows since $[\mu^X]_i = \frac{1}{N_{\text{div},x}} = \frac{\Delta x}{L}$, for $i \in \{1, \cdots, N_{\text{div},x}\}$. ■

Note that p_{cross} is a linear function of d_{step}, as expected. Since there are N people in the workspace, we can have simultaneous crosses.

Corollary 1: Let $p_{K,N}$ denote the PMF of random variable K denoting the number of simultaneous crosses with N people in the workspace. Assuming independent motion models for the people then results in the following expression

$$\begin{aligned}
p_{K,N}(k) &= \Pr(k \text{ simultaneous cross}) \\
&= \binom{N}{k} p_{\text{cross}}^k (1 - p_{\text{cross}})^{N-k},
\end{aligned} \tag{13}$$

where p_{cross} is as defined in Theorem 1.

Remark 2: Although, our derivation of p_{cross} is under the assumption of a constant speed d_{step}, our result can be extended to the case of a person moving with a variable random speed. Due to p_{cross} being linear in d_{step}, the probability of a cross would then become $p_{\text{cross}} = \frac{2\overline{d_{\text{step}}}}{\pi L}$, where $\overline{d_{\text{step}}}$ denotes the average speed of the person.

B. Derivation of the PDF of the received signal

In this section, we consider both blocking and MP effects and find an expression for the PDF of the received signal strength as a function of N.

Consider N people walking in the area of interest with a constant speed. As we discussed earlier, each person impacts the received signal by 1) blocking when she crosses the LOS and 2) scattering. Furthermore, there may be several other objects in the area impacting the received signal. We

assume that these objects are stationary in our modeling.[5] The baseband equivalent received signal is then given by

$$\begin{aligned} A &= \underbrace{b_0 e^{j\psi_0}}_{\text{LOS}} + \underbrace{\sum_{j=1}^{M} b_j e^{j\psi_j}}_{\text{MP due to static objects}} + \underbrace{\sum_{i=1}^{N} a_i e^{j\phi_i}}_{\text{MP due to walking people}}, \\ &= a_0 e^{j\phi_0} + \sum_{i=1}^{N} a_i e^{j\phi_i} \\ &= A_{\text{LOS,ST}} + A_{\text{MP}}, \end{aligned} \tag{14}$$

where b_0 and ψ_0 are the amplitude and phase of the LOS path respectively, a_i and ϕ_i are the amplitude and phase of the path resulting from scattering off of the i^{th} person respectively, and b_j and ψ_j, for $j \neq 0$, are the amplitude and phase of the path resulting from scattering off of the j^{th} static object respectively. Then $\sum_{j=1}^{M} b_j e^{j\psi_j}$ denotes the impact of other static objects on the received signal, with M representing the total number of such static objects. Let $A_{\text{LOS,ST}} \triangleq b_0 e^{j\psi_0} + \sum_{j=1}^{M} b_j e^{j\psi_j} = a_0 e^{j\phi_0}$ denote the summation of the LOS component and the MP due to the static objects. Furthermore, let $A_{\text{MP}} \triangleq \sum_{i=1}^{N} a_i e^{j\phi_i}$ represent the MP component due to people walking. The phase of each path, ϕ_i, for $i = 1, 2...N$, and ψ_j, for $j = 0, 1, 2...M$, is assumed to be uniformly distributed in $[0\ 2\pi]$.[6] ϕ_i is assumed independent of a_i and ϕ_j, and a_i is taken independent of a_j, for $j \neq i$ [27]. Note that the Doppler shifts due to the scatterer motion is small and thus not considered in this paper.

We are interested in deriving the PDF of the received signal amplitude $|A|$. Since $A_{\text{LOS,ST}}$ and A_{MP} are independent, we have [26]

$$C_A(U) = C_{A_{\text{LOS,ST}}}(U) C_{A_{\text{MP}}}(U),$$

where $C_{A_{\text{LOS,ST}}}(U)$, $C_{A_{\text{MP}}}(U)$ are the characteristic functions of $A_{\text{LOS,ST}}$ and A_{MP} respectively, and U is the corresponding variable of the characteristic functions.

$C_{A_{\text{MP}}}(U)$ can be characterized as follows:

$$\begin{aligned} C_{A_{\text{MP}}}(U) &= \mathrm{E}_{A_{\text{MP}}}(e^{jU \bullet A_{\text{MP}}}) \\ &= \mathrm{E}_{A_{\text{MP}}}(e^{jU \bullet (\sum_{i=1}^{N} a_i e^{j\phi_i})}) \\ &= \mathrm{E}_{A_{\text{MP}}}(\prod_{i=1}^{N} e^{jU \bullet (a_i e^{j\phi_i})}) \\ &= \prod_{i=1}^{N} \mathrm{E}_{a_i,\phi_i}(e^{jU \bullet (a_i e^{j\phi_i})}) \\ &\qquad \text{(since } a_i, \phi_i \text{ independent of } a_j, \phi_j) \\ &= \prod_{i=1}^{N} \mathrm{E}_{a_i,\phi_i}(e^{j|U| a_i cos(\phi_i - \angle(u))}) \\ &= \prod_{i=1}^{N} \mathrm{E}_{a_i}(J_0(a_i|U|)), \end{aligned} \tag{15}$$

where J_0 is the zeroth-order Bessel function of the first kind, $\mathrm{E}_a(.)$ represents the expectation w.r.t a, and $\bullet$ represents the dot product. Similarly, the characteristic function of $A_{\text{LOS,ST}}$ is given by

$$C_{A_{\text{LOS,ST}}}(U) = \mathrm{E}_{a_0}(J_0(a_0|U|)). \tag{16}$$

Note that the characteristic functions depend only on the magnitude of U and therefore are circular symmetric [27]. The PDF of A is then given as

$$\begin{aligned} p_A(Z) &= \frac{1}{4\pi^2} \int_{|U|=0}^{\infty} \int_{\angle U=0}^{2\pi} e^{-jU \bullet Z} C_A(U) |U| d|U| d\angle U \\ &= \frac{1}{4\pi^2} \int_{|U|=0}^{\infty} \int_{\angle U=0}^{2\pi} e^{-j|U||Z|\cos(\angle U - \angle Z)} C_A(U) |U| d|U| d\angle U \\ &= \frac{1}{4\pi^2} \int_{|U|=0}^{\infty} |U| \Big(\int_{\angle U=0}^{2\pi} e^{-j|U||Z|\cos(\angle U - \angle Z)} d\angle U \Big) \\ &\qquad C_A(U) d|U| \\ &= \frac{1}{2\pi} \int_{|U|=0}^{\infty} |U| J_0(|U||Z|) C_A(U) d|U| \\ &= \frac{1}{2\pi} \int_{|U|=0}^{\infty} |U| J_0(|U||Z|) \Big(\prod_{i=1}^{N} \mathrm{E}_{a_i}(J_0(a_i|U|)) \Big) \\ &\qquad \mathrm{E}_{a_0}(J_0(a_0|U|)) d|U|. \end{aligned} \tag{17}$$

Then, the PDF of $|A|$ can be found as

$$\begin{aligned} p_{|A|}(z) &= \int_{\angle A=0}^{2\pi} z p_A(A) d\angle A \\ &= z \int_{|U|=0}^{\infty} |U| J_0(|U|z) \Big(\prod_{i=1}^{N} \mathrm{E}_{a_i}(J_0(a_i|U|)) \Big) \\ &\qquad \mathrm{E}_{a_0}(J_0(a_0|U|)) d|U|. \end{aligned} \tag{18}$$

Random variable a_0 can only take discrete values corresponding to the received signal strength when different number of people are along the LOS path. Thus by using Theorem 1, we have the following for the PDF of a_0 [7]

$$p_{a_0} = \sum_{k=0}^{N} \binom{N}{k} p_{\text{cross}}^k (1 - p_{\text{cross}})^{N-k} \delta(a_0 - B_k), \tag{19}$$

where B_k is the received signal amplitude when k people are along the LOS path,[8] and $\delta(.)$ is the Dirac delta function. Using (19), we get

$$\mathrm{E}_{a_0}(J_0(a_0|U|)) = \sum_{k=0}^{N} \binom{N}{k} p_{\text{cross}}^k (1 - p_{\text{cross}})^{N-k} J_0(|U|B_k). \tag{20}$$

In order to evaluate the characteristic function of A_{MP}, we need to characterize the PDF of a_i for $i \neq 0$, i.e. the amplitude of each component of MP due to people walking. Since a_i for $i \neq 0$ is the amplitude of the scattered signal from only one scatterer (one person), Rayleigh statistics cannot be used [27]. In a different context, a K-distribution is widely used to model the sea clutter and echo signal from biological tissues when the number of scatterers are low [27], [28], [29]. We thus use

[5] During the experiment, other surrounding objects such as leaves may move. However, the impact of their motion is typically negligible as compared to other effects.

[6] This assumption is justifiable since we operate at a high frequency [26].

[7] Note that this is the PDF of the received signal amplitude when there is no MP component due to people walking, i.e. only the LOS component and MP due to static objects are present.

[8] Note that impact of static objects is inherently included in B_k.

K-distribution to model the PDF of a_i for $i \neq 0$ as follows [27],

$$p_{a_i} = \frac{2b}{\Gamma(1+\nu)}\Big(\frac{ba}{2}\Big)^{\nu+1} K_\nu(ba) \quad \nu > -1, i \neq 0 \qquad (21)$$

where $K_\nu(.)$ is the modified Bessel function of the second kind, and b and ν are the parameters of the distribution. Since the scatterers are taken to have identical statistics, we get

$$\prod_{i=1}^{N} \mathrm{E}_{a_i}(J_0(a_i|U|)) = (\mathrm{E}_{a_i}(J_0(a_i|U|)))^N. \qquad (22)$$

Therefore the PDF of $|A|$ is given by

$$\begin{aligned} p_{|A|,N}(z) &= z\int_{|U|=0}^{\infty} |U| J_0(|U|z)(\mathrm{E}_{a_i}(J_0(a_i|U|)))^N \mathrm{E}_{a_0}(J_0(a_0|U|))d|U| \\ &= z\int_{|U|=0}^{\infty} |U| J_0(|U|z) f(N) d|U|, \end{aligned} \qquad (23)$$

where we added the subscript N to emphasize the dependency on N, and

$$f(N) = (\mathrm{E}_{a_i}(J_0(a_i|U|)))^N \mathrm{E}_{a_0}(J_0(a_0|U|)). \qquad (24)$$

IV. Experimental Results

In this section, we show that our proposed framework can estimate the number of people well in several different cases in both indoor and outdoor environments. We start by briefly summarizing our experimental setup.

We use an 802.11g card for both the transmitter and the receiver. More specifically, the transmitter uses D-Link WBR-1310 wireless router [30], broadcasting a wireless signal. The receiver then constantly measures its receptions. In our setup, the transmitter and receiver are stationary and mounted on two Pioneer 3-AT mobile robots from MobileRobots Inc. [31], as shown in Fig. 4a. It should be noted that any other object could have been used to hold the TX/RX as far as the scenario of this paper is concerned (since the TX and RX are not moving). However, the automation through the use of robots hold promises for the future extensions of this work. The overall operation is then overseen by a remote PC, which is in charge of communicating the execution plan and collecting the final received signal strength (RSS) readings at the end of the operation.

We run two different sets of experiments in both outdoor and indoor environments. In the first set of experiments, we use directional antennas for both the transmitter and the receiver. We then show that in this case, modeling the received signal with only $A_{\text{LOS,ST}}$ of (14) suffices for the estimation of the number of people. In the second case, we use omnidirectional antennas at both the transmitter and the receiver. We then show that a good estimation of the total number of people can be achieved by using our proposed modeling of (23).

Fig. 5a shows the outdoor site, which has the dimensions $L = 7$ m and $B = 10$ m. Fig. 5b then shows the indoor site with the dimensions $L = 4.4$ m and $B = 7.5$ m. These dimensions are assumed to be known to the estimator. Experiments are carried out with 1, 3, 5, 7 and 9 people. People are told to walk casually in the area and bounce of the boundary when they approach it. The data is collected for 300 seconds, at the rate of 50 samples/s. A constant velocity of 1 m/s is assumed for the estimation process. Note that this is only for the purpose of mathematical modeling and estimation, and that we have no control over the speed of the people when they walk.

(a)

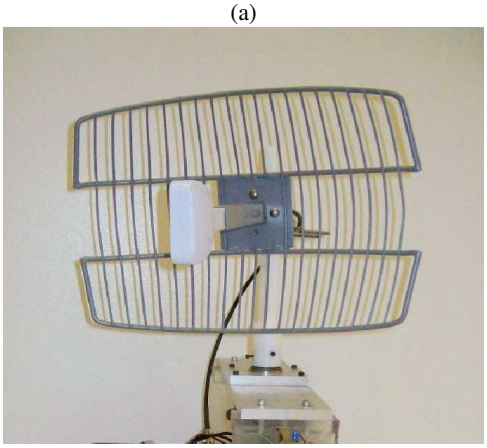

(b)

Fig. 4: (a) Pioneer 3-AT Robot with an omnidirectional antenna, (b) GD24-15 2.4 GHz parabolic grid directional antenna.

The environment of interest has other objects that will interact with the transmitted signal,[9] as discussed in (14), and their impact is modeled in $A_{\text{LOS,ST}}$. As can be seen from (23), prior estimation of B_ks is needed for our approach. In order to acquire this, prior measurements are made when k number of people are walking on the straight line connecting the transmitter and the receiver (in order to average the attenuation over several possible combinations). We should note that in practice this approach is scalable for the following reason. As the number of people increases, the value of B_k starts to saturate. Thus, we only need to collect prior measurements in order to estimate B_k for the lower values of k. In addition, dynamical system models can also be utilized to further fine tune the estimation of B_k at the higher values of k. Let $\widehat{B_k}$ represent the prior estimation of B_k in the rest of this section.

[9]We assume that these objects are not moving. However, when we carry out our experiments, movements of vehicles and leaves (in the outdoor environment) were naturally inevitable.

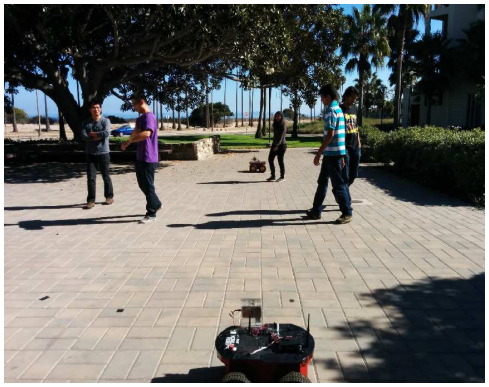

(a) Outdoor Site

(b) Indoor site

Fig. 5

As for the MP part (A_{MP} in (14)), we further need a prior estimation of b and ν. We measure these parameters a priori by having one person move in the area without crossing the LOS path. Then, the PDF of the collected measurements is matched to the convolution of the K-distribution of (21) and the PDF of the LOS path when no people are around, in order to find the best fit of b and ν.

A. Estimation of the Number of People in Outdoor Environments

In this section, we show our results in outdoor environments with both directional and omnidirectional antennas.

1) Estimation with Directional Antennas: In this part, directional antennas are used at both the transmitter and the receiver. More specifically, we use GD24-15 2.4 GHz parabolic grid antennas from Laird Technologies, as shown in Fig. 4b. This model has a 15 dBi gain with 21 degree horizontal and 17 degree vertical beamwidth and is suitable for IEEE 802.11 b/g applications [32]. This is an important case to study as it brings an understanding to the blocking characterization of Section III-A (first term in the second equation of (14)). More specifically, we see that, in this case, the impact of the crowd on the transmitted signal is mainly captured through the first term in (14), i.e. people impact the signal when they cross the LOS, and the multipath effect, due to scattering off of people, is negligible.

From (13), we have $p_{K,N}$, the theoretical PMF for the number of simultaneous crosses per time, as a function of

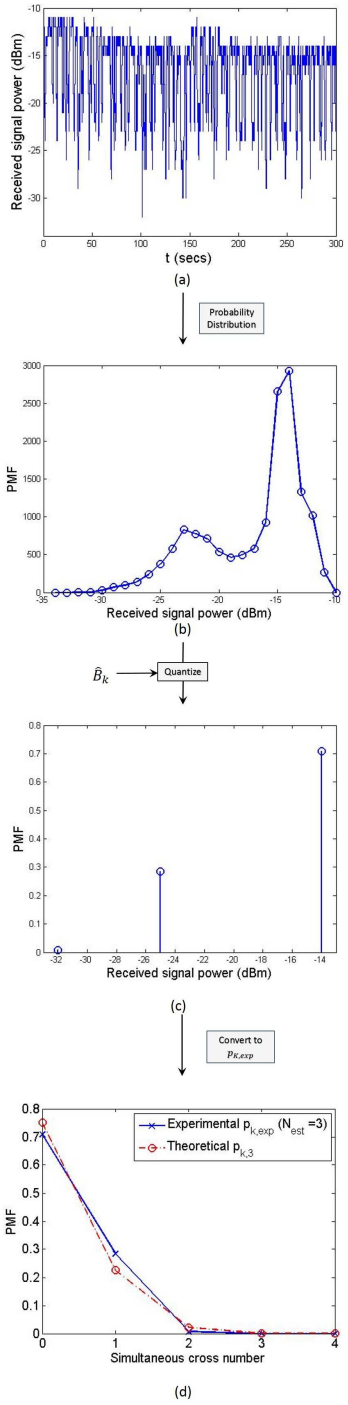

Fig. 6: An illustration of our approach for estimating N in the directional case.

N. Since we are not considering the impact of MP due to people walking in this case, this equation will be the base for our estimation of N. Fig. 6 summarizes the underlying estimation steps in this case. Fig. 6a shows an example of the received signal power measured for a sample case of $N = 3$ in the outdoor environment. First, we generate the PMF of the measured RSS (Fig. 6b). By using $\widehat{B_k}$s, the prior estimates of B_ks, the PMF is quantized to the closest $\widehat{B_k}$s (Fig. 6c), which can then be directly translated into an estimation of the

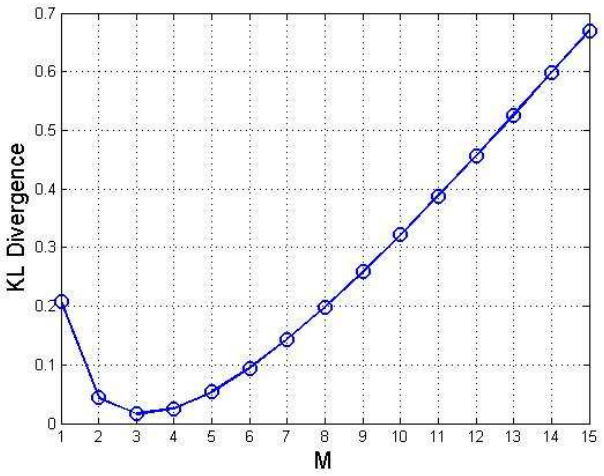

Fig. 7: KL divergence $D_{\text{KL}}(p_{K,\text{exp}}||p_{K,M})$ between the theoretical and experimental PMF of simultaneous crosses, as a function of M, for the case of $N = 3$ (with directional antennas) in the outdoor site. It can be seen that the curve is minimized at $N_{\text{est}} = 3$, resulting in an accurate estimation of the total number of people.

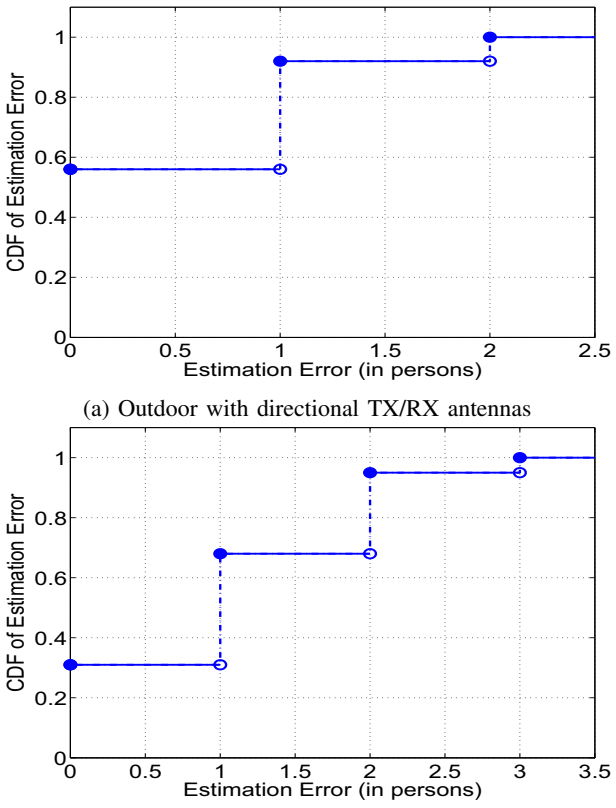

(a) Outdoor with directional TX/RX antennas

(b) Outdoor with omnidirectional TX/RX antennas

Fig. 8: The CDF of the estimation error for the case of (a) directional TX/RX and (b) omnidirectional TX/RX antennas in the outdoor environment, based on several experiments with up to and including 9 people. It can be seen that we can estimate the total number of people with a good accuracy.

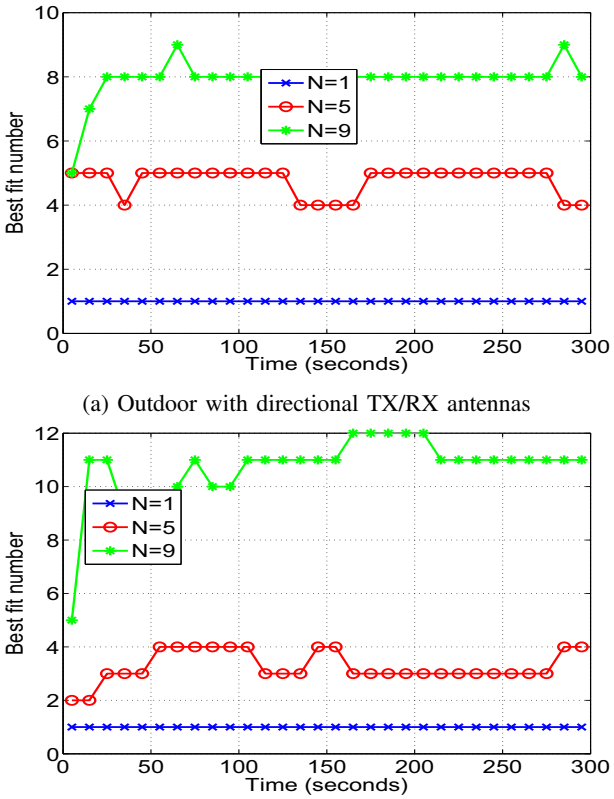

(a) Outdoor with directional TX/RX antennas

(b) Outdoor with omnidirectional TX/RX antennas

Fig. 9: Sample occupancy estimations, as a function of time, for the case of (a) directional TX/RX and (b) omnidirectional TX/RX antennas in the outdoor environment. It can be seen that the estimation converges to within 1 person of its final value in 100 seconds.

PMF of K (the number of simultaneous crosses) (Fig. 6d). Let $p_{K,\text{exp}}$ denote this estimated PMF. We then find $N_{\text{est,dir}}$ such that it minimizes the Kullback-Leibler (KL) divergence between the experimental and theoretical PMFs:

$$N_{\text{est,dir}} = \arg\min_{M} D_{\text{KL}}(p_{K,\text{exp}}||p_{K,M}), \tag{25}$$

where $D_{\text{KL}}(p_1||p_2)$ is the KL divergence [33] between the two distributions p_1 and p_2. Fig. 6d also shows the theoretical PMF of K for the case of three people. It can be seen that the curve is very close to the experimental one. Fig. 7 further shows the corresponding KL divergence curve as a function of M for a sample case for $N = 3$ in the outdoor environment. It can be seen that the curve is minimized at $N = 3$, resulting in the accurate estimation of N in this case.

Table I shows the performance of our approach for different number of people, for a sample case in the outdoor environment. It can be seen that our approach can estimate the number of people considerably well in this case. To see the variability of the results in different runs, we further run 5 experiments on 5 different days for each number of occupants indicated in the first row of Table I. Fig. 8a show the resulting Cumulative Distribution Function (CDF) of the estimation error of all the cases (5 runs) in terms of the number of people for the outdoor

case and with directional antennas. It can be seen that, the estimation error is 0 or 1 person 92% of the time and 2 or less 100% of the time.

Number of People in the Area	1	3	5	7	9
Estimated Number of People	1	3	4	7	8

TABLE I: Sample performance of our approach for the case of directional antennas in the outdoor environment.

So far, we have presented our results based on the collected measurements of 300 seconds. In order to see the impact of the measurement time on the estimation error, Fig. 9a further shows occupancy estimation, as a function of time, for three sample experiments in the outdoor environment. It can be seen that the estimation converges to within an error of 1 of its final value after 100 seconds for these sample cases. This suggests that a shorter time duration could have also resulted in a similar performance in these cases. In general, the time duration should be chosen such that the experiment has reached its steady state. An upper bound for this time duration can be obtained based on the size of the area, the assumed walking speed, and an upper bound on the expected number of people.

2) Estimation with Omnidirectional Antennas: In this scenario, omnidirectional antennas are used at both the transmitter and the receiver. Thus, both LOS and MP components need to be considered, which makes the estimation process more challenging. The PDF of the received signal amplitude is as derived in (23), which is an implicit function of N. Let p_{exp} represent the PDF of the measured received signal amplitude. Then, we estimate the total number of people through the following KL divergence minimization:

$$N_{\text{est,omni}} = \arg\min_{M} D_{\text{KL}}(p_{\text{exp}} || p_{|A|,M}). \tag{26}$$

Table II shows the performance of our approach for different number of people for a sample case in the outdoor environment. It can be seen that the estimation performance is considerably good for this sample case. To see the variability of the results in different runs, we further run 5 experiments on 5 different days for each number of occupants indicated in the first row of Table II. Fig. 8b shows the resulting Cumulative Distribution Function (CDF) of the estimation error of all the cases (5 runs) in terms of the number of people.

It can be seen that the estimation error is 2 or less 96% of the time, which is a good accuracy. As expected, probability of error is higher as compared to Fig. 8a where directional antennas were used. Fig. 9b shows occupancy estimation, as a function of time, for sample experiments with omnidirectional antennas. It can be seen that the estimation converges to within an error of 1 of its final value after 100 seconds for these cases as well. Finally, Fig. 10 compares the corresponding experimental and theoretical PDFs for sample cases with different number of people. Each plot shows the amplitude PDF of the experimental data and the best fit theoretical PDF obtained by minimizing the KL divergence. The resulting N is then shown as $N_{\text{est,omni}}$. It can be seen that the experimental and theoretical pdfs are matching well.

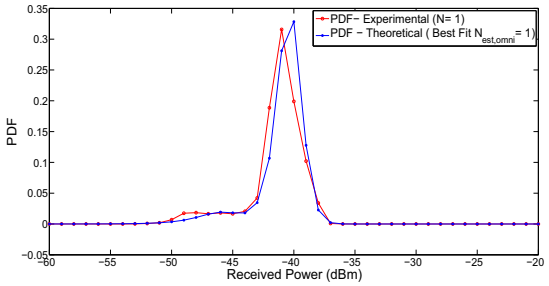

(a) N=1

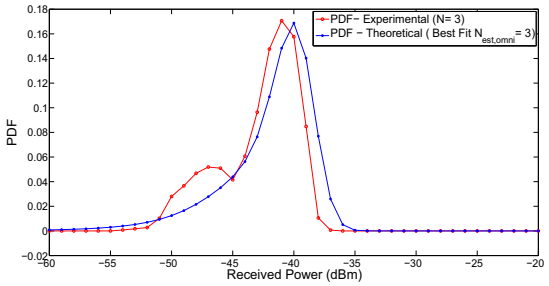

(b) N=3

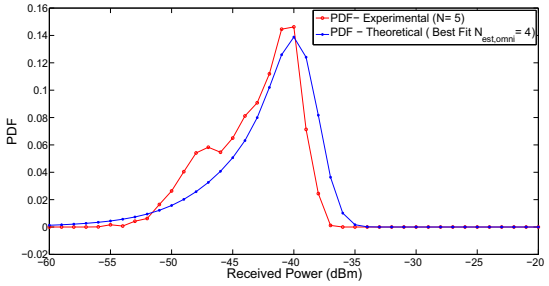

(c) N=5

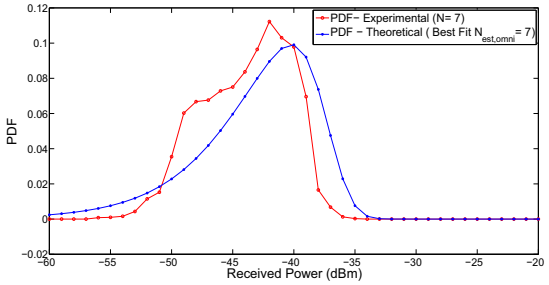

(d) N=7

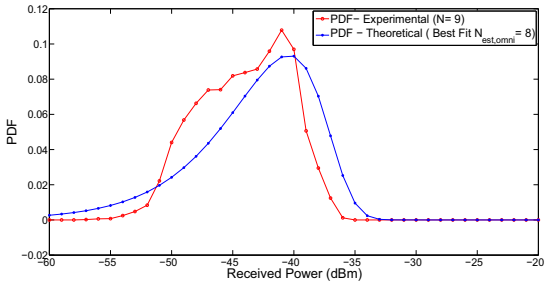

(e) N=9

Fig. 10: A Comparison of the theoretical PDF of (23) and the experimental PDF for different cases (with omnidirectional antennas) in the outdoor environment.

Number of people in the Area	1	3	5	7	9
Estimated Number of People	1	3	4	7	8

TABLE II: Sample performance of our approach for the case of omnidirectional antennas in the outdoor environment.

B. Estimation of the Number of People in Indoor Environments

In this section, we show our results for estimating the level of occupancy in indoor. The site details are shown in Fig. 5b and summarized earlier in Section IV. The rest of the experimental setup is the same as for the outdoor case. As expected, the indoor environment will experience more multipath effect due to static objects. Our results indicate that we can still estimate the total number of people with a good accuracy.

1) Estimation with Directional Antennas: Table III shows the performance of our approach for different number of people for a sample case in the indoor site when directional antennas are used. In this case, (19) suffices to estimate the number of people, as discussed earlier. It can be seen that our approach can estimate the level of occupancy well in an indoor setting. To see the variability of the results in different runs, we further run 7 experiments on 7 different days for each number of occupants indicated in the first row of Table III. Fig. 11a then shows the resulting Cumulative Distribution Function (CDF) of the estimation error of all the cases (7 runs) in terms of the number of people for the indoor site. It can be seen that the estimation error is 0 or 1 88% of the time and 2 or less 100% of time, showing a good performance.

Remark 3: In this paper, we have observed a good estimation performance with only considering the LOS and static objects for the directional case. However, since a typical directional antenna will still measure some of the scattering off of walking people, further improvement can possibly be achieved if the whole proposed expression of Section III-B is also utilized for the directional case.

Number of People in the Area	1	3	5	7	9
Estimated Number of People	1	3	4	6	7

TABLE III: Sample performance of our approach for the case of directional antennas in the indoor environment.

2) Estimation with Omnidirectional Antennas: Next, we test our proposed approach with omnidirectional antennas in the indoor site of Section III-B). Table IV shows the performance of our approach for different number of people for a sample case. It can be seen that our approach can also estimate the level of occupancy well in an indoor setting with omnidirectional antennas. To see the variability of the results in different runs, we further run 7 experiments on 7 different days for each number of occupants indicated in the first row of Table IV. Fig. 11b then shows the resulting Cumulative Distribution Function (CDF) of the estimation error of all the cases (7 runs) in terms of the number of people. It can be seen that the estimation error is 2 or less 63% of time, confirming a successful indoor performance with typical omnidirectional antennas that come as part of the 802.11 WLAN cards.

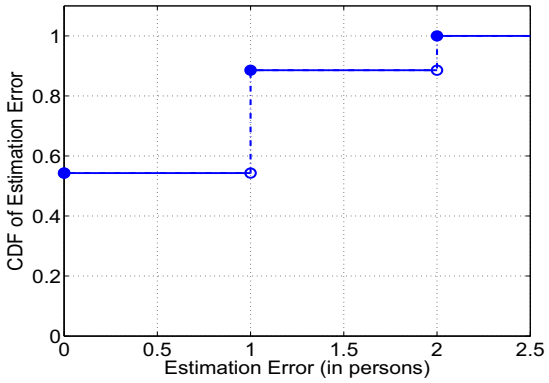

(a) Indoor with directional TX/RX antennas

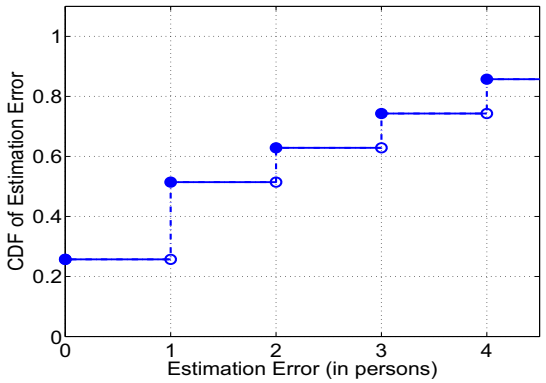

(b) Indoor with omnidirectional TX/RX antennas

Fig. 11: The CDF of the estimation error for the case of (a)directional TX/RX and (b)omnidirectional TX/RX antennas in the indoor environment, based on several experiments with up to and including 9 people. It can be seen that we can estimate the total number of people with a good accuracy.

Number of people in the Area	1	3	5	7	9
Estimated Number of People	2	3	8	10	11

TABLE IV: Sample performance of our approach for the case of omnidirectional antennas in the indoor environment.

C. Final Remarks on the Experimental Results

Our results confirmed that our proposed approach can successfully estimate the level of occupancy in both indoor and outdoor environments with typical WLAN cards and omnidirectional antennas, based on only WiFi power measurements. As expected, if directional antennas are available, the performance can further be improved by limiting the multipath fading effects.

V. Conclusions

In this paper, we proposed a new approach for estimating the total number of people walking in an area with only WiFi power measurements between a pair of stationary transmitter/receiver antennas. More specifically, we separated the impact of the crowd on the transmitted signal into two key components: 1) blocking of the LOS and 2) MP effects caused by scattering. By developing a simple motion model, we first mathematically characterized the impact of the crowd

on blocking the LOS. We further probabilistically characterized the resulting multipath fading and developed an overall mathematical expression for the probability distribution of the received signal amplitude as a function of the total number of occupants, which was the base for our estimation using KL Divergence. In order to confirm our approach, we ran several indoor and outdoor experiments with up to and including 9 people and showed that the proposed framework can estimate the total number of people with a good accuracy.

VI. Acknowledgements

The authors would like to thank the students that walked for our experiments. Furthermore, the authors would like to thank Dr. Bamieh and Dr. Eisenhower for useful discussions on the application of this work for heating and cooling optimization.

References

[1] Alejandro Gonzalez-Ruiz, Alireza Ghaffarkhah, and Yasamin Mostofi. An integrated framework for obstacle mapping with see-through capabilities using laser and wireless channel measurements. *IEEE SENSORS JOURNAL*, 14(1):25–38, 2014.

[2] He Wang, Souvik Sen, Ahmed Elgohary, Moustafa Farid, Moustafa Youssef, and Romit Roy Choudhury. No need to war-drive: unsupervised indoor localization. In *Proceedings of the 10th international conference on Mobile systems, applications, and services*, pages 197–210. ACM, 2012.

[3] Dian Zhang, Yanyan Yang, Dachao Cheng, Siyuan Liu, and Lionel M Ni. Cocktail: an RF-based hybrid approach for indoor localization. In *Communications (ICC), 2010 IEEE International Conference on*, pages 1–5. IEEE, 2010.

[4] Yasamin Mostofi. Cooperative wireless-based obstacle/object mapping and see-through capabilities in robotic networks. *Mobile Computing, IEEE Transactions on*, 12(5):817–829, 2013.

[5] Fadel Adib, Zachary Kabelac, and Dina Katabi. Multi-person motion tracking via rf body reflections. 2014.

[6] Joey Wilson and Neal Patwari. See-through walls: Motion tracking using variance-based radio tomography networks. *Mobile Computing, IEEE Transactions on*, 10(5):612–621, 2011.

[7] Qifan Pu, Sidhant Gupta, Shyamnath Gollakota, and Shwetak Patel. Whole-home gesture recognition using wireless signals. In *Proceedings of the 19th annual international conference on Mobile computing & networking*, pages 27–38. ACM, 2013.

[8] Yuvraj Agarwal, Bharathan Balaji, Rajesh Gupta, Jacob Lyles, Michael Wei, and Thomas Weng. Occupancy-driven energy management for smart building automation. In *Proceedings of the 2nd ACM Workshop on Embedded Sensing Systems for Energy-Efficiency in Building*, pages 1–6. ACM, 2010.

[9] Tuan Anh Nguyen and Marco Aiello. Energy intelligent buildings based on user activity: A survey. *Energy and buildings*, 56:244–257, 2013.

[10] Minjin Kim, Wonjun Kim, and Changick Kim. Estimating the number of people in crowded scenes. In *IS&T/SPIE Electronic Imaging*, pages 78820L–78820L. International Society for Optics and Photonics, 2011.

[11] Sheng-Fuu Lin, Jaw-Yeh Chen, and Hung-Xin Chao. Estimation of number of people in crowded scenes using perspective transformation. *Systems, Man and Cybernetics, Part A: Systems and Humans, IEEE Transactions on*, 31(6):645–654, 2001.

[12] Min Li, Zhaoxiang Zhang, Kaiqi Huang, and Tieniu Tan. Estimating the number of people in crowded scenes by mid based foreground segmentation and head-shoulder detection. In *Pattern Recognition, 2008. ICPR 2008. 19th International Conference on*, pages 1–4. IEEE, 2008.

[13] Lionel M Ni, Yunhao Liu, Yiu Cho Lau, and Abhishek P Patil. LANDMARC: indoor location sensing using active rfid. *Wireless networks*, 10(6):701–710, 2004.

[14] Pravein Govindan Kannan, Seshadri Padmanabha Venkatagiri, Mun Choon Chan, Akhihebbal L Ananda, and Li-Shiuan Peh. Low cost crowd counting using audio tones. In *Proceedings of the 10th ACM Conference on Embedded Network Sensor Systems*, pages 155–168. ACM, 2012.

[15] Jens Weppner and Paul Lukowicz. Bluetooth based collaborative crowd density estimation with mobile phones. In *Pervasive Computing and Communications (PerCom), 2013 IEEE International Conference on*, pages 193–200. IEEE, 2013.

[16] Yaoxuan Yuan, Chen Qiu, Wei Xi, and Jizhong Zhao. Crowd density estimation using wireless sensor networks. In *Mobile Ad-hoc and Sensor Networks (MSN), 2011 Seventh International Conference on*, pages 138–145. IEEE, 2011.

[17] Chenren Xu, Bernhard Firner, Robert S Moore, Yanyong Zhang, Wade Trappe, Richard Howard, Feixiong Zhang, and Ning An. SCPL: Indoor device-free multi-subject counting and localization using radio signal strength. In *Proceedings of the 12th international conference on Information Processing in Sensor Networks*, pages 79–90. ACM, 2013.

[18] Moustafa Seifeldin, Ahmed Saeed, Ahmed E Kosba, Amr El-Keyi, and Moustafa Youssef. Nuzzer: A large-scale device-free passive localization system for wireless environments. *Mobile Computing, IEEE Transactions on*, 12(7):1321–1334, 2013.

[19] M. Nakatsuka, H. Iwatani, and J. Katto. A study on passive crowd density estimation using wireless sensors.

[20] Wei Xi, Jizhong Zhao, Xiang-Yang Li, Kun Zhao, Shaojie Tang, Xue Liu, and Zhiping Jiang. Electronic frog eye: Counting crowd using wifi.

[21] Hao Lv, Miao Liu, Teng Jiao, Yang Zhang, Xiao Yu, Sheng Li, Xijing Jing, and Jianqi Wang. Multi-target human sensing via uwb bio-radar based on multiple antennas. In *TENCON 2013-2013 IEEE Region 10 Conference (31194)*, pages 1–4. IEEE, 2013.

[22] Jin He and Anish Arora. A regression-based radar-mote system for people counting. In *Pervasive Computing and Communications (PerCom), 2014 IEEE International Conference on*, pages 95–102. IEEE, 2014.

[23] Henryk Minc. *Nonnegative matrices*. Wiley, 1988.

[24] Carl D Meyer. *Matrix analysis and applied linear algebra*. Siam, 2000.

[25] Christopher David Godsil, Gordon Royle, and CD Godsil. *Algebraic graph theory*, volume 207. Springer New York, 2001.

[26] Andrea Goldsmith. *Wireless communications*. Cambridge university press, 2005.

[27] Eo Jakeman and PN Pusey. A model for non-rayleigh sea echo. *Antennas and Propagation, IEEE Transactions on*, 24(6):806–814, 1976.

[28] E Jakeman and RJA Tough. Generalized k distribution: a statistical model for weak scattering. *JOSA A*, 4(9):1764–1772, 1987.

[29] P Mohana Shankar. Ultrasonic tissue characterization using a generalized nakagami model. *Ultrasonics, Ferroelectrics and Frequency Control, IEEE Transactions on*, 48(6):1716–1720, 2001.

[30] D-link. http://www.dlink.com.

[31] MobileRobots Inc. http://www.mobilerobots.com.

[32] Laird Technologies. http://www.lairdtech.com/Products/Antennas-and-Reception-Solutions/.

[33] Thomas M Cover and Joy A Thomas. *Elements of information theory*. John Wiley & Sons, 2012.

Saandeep Depatla received the Bachelors degree in Electronics and Communication Engineering from the National Institute of Technology, Warangal in 2010 and the MS degree in Electrical and Computer Science Engineering (ECE) from the University of California, Santa Barbara (UCSB) in 2014. From 2010 to 2012 he worked on developing antennas for radars in Electronics and Radar Development Establishment, India. Since 2013, he has been working towards his Ph.D. degree in ECE at UCSB. His research interests include signal processing, wireless communications and electromagnetics.

Arjun Muralidharan received the Bachelors degree in Electronics and Communication Engineering from the Indian Institute of Technology, Guwahati, in 2012 and the MS degree in Electrical and Computer Science Engineering (ECE) from the University of California, Santa Barbara (UCSB) in 2014. He is currently working towards his PhD degree in the Department of Electrical and Computer Engineering at the University of California Santa Barbara. His research interests include cooperative robotic networks, game theory, wireless communications and information theory.

Yasamin Mostofi received the B.S. degree in electrical engineering from Sharif University of Technology, Tehran, Iran, in 1997, and the M.S. and Ph.D. degrees in the area of wireless communications from Stanford University, California, in 1999 and 2004, respectively. She is currently an associate professor in the Department of Electrical and Computer Engineering at the University of California Santa Barbara. Prior to that, she was a faculty in the Department of Electrical and Computer Engineering at the University of New Mexico from 2006 to 2012. She was a postdoctoral scholar in control and dynamical systems at the California Institute of Technology from 2004 to 2006. Dr. Mostofi is the recipient of the Presidential Early Career Award for Scientists and Engineers (PECASE), the National Science Foundation (NSF) CAREER award, and IEEE 2012 Outstanding Engineer Award of Region 6 (more than 10 western states). She also received the Bellcore fellow-advisor award from Stanford Center for Telecommunications in 1999 and the 2008-2009 Electrical and Computer Engineering Distinguished Researcher Award from the University of New Mexico. Her research is on mobile sensor networks. Current research thrusts include RF sensing, see-through imaging with WiFi, X-ray vision for robots, communication-aware robotics, and robotic networks. Her research has appeared in several news outlets such as BBC and Engadget. She has served on the IEEE Control Systems Society conference editorial board 2008-2013. She is currently an associate editor for the IEEE TRANSACTIONS ON CONTROL OF NETWORK SYSTEMS. She is a senior member of the IEEE.